

# Exploring Decision-based Black-box Attacks on Face Forgery Detection

Zhaoyu Chen, *Graduate Student Member, IEEE*, Bo Li, Kaixun Jiang,  
Shuang Wu, Shouhong Ding, Wenqiang Zhang, *Member, IEEE*

**Abstract**—Face forgery generation technologies generate vivid faces, which have raised public concerns about security and privacy. Many intelligent systems, such as electronic payment and identity verification, rely on face forgery detection. Although face forgery detection has successfully distinguished fake faces, recent studies have demonstrated that face forgery detectors are very vulnerable to adversarial examples. Meanwhile, existing attacks rely on network architectures or training datasets instead of the predicted labels, which leads to a gap in attacking deployed applications. To narrow this gap, we first explore the decision-based attacks on face forgery detection. However, applying existing decision-based attacks directly suffers from perturbation initialization failure and low image quality. First, we propose cross-task perturbation to handle initialization failures by utilizing the high correlation of face features on different tasks. Then, inspired by using frequency cues by face forgery detection, we propose the frequency decision-based attack. We add perturbations in the frequency domain and then constrain the visual quality in the spatial domain. Finally, extensive experiments demonstrate that our method achieves state-of-the-art attack performance on FaceForensics++, CelebDF, and industrial APIs, with high query efficiency and guaranteed image quality. Further, the fake faces by our method can pass face forgery detection and face recognition, which exposes the security problems of face forgery detectors.

**Index Terms**—Adversarial examples, Face forgery detection, Black-box attacks, Face recognition

## I. INTRODUCTION

With the success of deep neural networks [1]–[5] and the development of generative models [6]–[9], face forgery generation has made excellent progress. We can synthesize highly realistic fake faces by these techniques, such as Face2Face [10], FaceSwap [11], DeepFakes [12] and NeuralTextures [13]. Further, methods such as StyleGAN [14] edit one’s attributes (hair, glasses, age, etc.) to generate various faces, and these faces are widely used in scenes such as the film industry and virtual uploaders. In contrast, these fake faces also lead to the spread of false news or damage to reputation, raising public concerns about security and privacy [15]. Therefore, researchers have recently focused on how to design effective face forgery detection methods to determine whether a face has been modified.

Face forgery detection is usually defined as a binary classification problem, distinguishing between real and fake faces.

Zhaoyu Chen, Kaixun Jiang, and Wenqiang Zhang are with Academy for Engineering and Technology, Fudan University, Shanghai, China, and also with Yiwu Research Institute of Fudan University, Yiwu, China. The emails of these authors are: zhaoyuchen20@fudan.edu.cn.

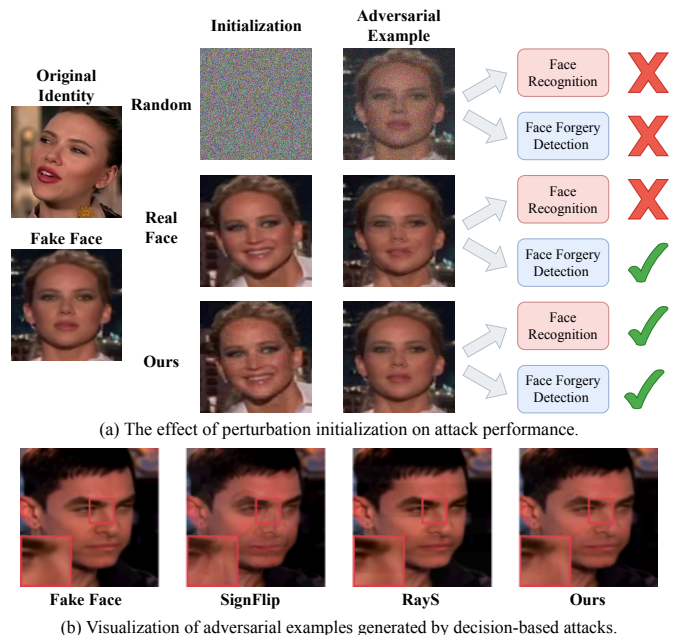


Fig. 1. When directly using existing decision-based attacks on face forgery detection, it is prone to (a) *perturbation initialization failure* and (b) *low image quality*, which affects attack performance and limits the application of the face (i.e. simultaneously attacking face recognition and face forgery detection). ✓ represents recognition as the original identity or detection as real faces.

There is a series of face forgery detectors [1]–[4], [16], [17] proposed that utilize deep neural networks to automatically learn feature differences between real and fake faces and achieve remarkable success on multiple datasets [18], [19]. Despite their success, recent work [20] shows that face forgery detectors are very vulnerable to adversarial examples [21]–[23], which exposes the current shortcut of security in face forgery detection. After adding a carefully-designed adversarial perturbation, a face originally classified as the fake is recognized as real by face forgery detectors. Existing methods [20], [24]–[28] have explored the adversarial robustness of face forgery detection, but these methods require access to the detector’s network architecture or training datasets instead of the predicted labels. However, when attacking industrial APIs, we cannot access the details of the models or datasets, but only the decision (real or fake) returned by the service. Therefore, the lack of decision-based attacks leads to a gap in the robustness analysis of face forgery detection.

When exploring decision-based attacks on face forgery detection, it is easiest to apply existing decision-based attacks directly [29]–[34]. However, directly applying existing decision-based attacks to face forgery detection may encounter some issues: (a) *perturbation initialization failure*. Existing decision-based attacks usually adopt random noise as attack initialization. However, since adding noise itself is a kind of manipulation, faces with random noise are usually recognized as fake faces by face forgery detection (as shown in Fig. 1). (b) *low image quality*. For example, RayS [35] introduces perceptible regular rectangular perturbation. Using real faces as perturbation initialization [33] leads to artifacts and may affect the application of faces, e.g. face recognition, as shown in Fig. 1. Therefore, we need an efficient decision-based attack designed for face forgery detection to identify potential vulnerabilities on face forgery detection and provide insights on possible improvements.

To address these issues, we propose an efficient decision-based adversarial attack to explore the adversarial robustness of face forgery detection. First, we propose a cross-task perturbed initialization method to handle initialization failures of decision-based attacks on face forgery detection. Specifically, although it is difficult for us to obtain face forgery detectors because we do not know the face and its modification method, it is relatively easy to obtain many open-source face recognition models. With the high correlation of face features on two types of tasks, we generate cross-task adversarial perturbations in the face recognition model as initial perturbations to attack face forgery detection. Second, since the features of face forgery detection are highly discriminative in the frequency domain [16], [17], [36], we propose a frequency decision-based attack. After obtaining cross-task adversarial perturbations, we add perturbations to faces in the frequency domain and then constrain the visual quality in the spatial domain. Finally, our method achieves state-of-the-art attack performance on FaceForensics++ [18] and CelebDF [19], with high query efficiency and guaranteed image quality. We also successfully attack the real-world industrial API and showcase the effectiveness of our method in practice. Furthermore, fake faces by our method can simultaneously pass face forgery detection and face recognition, which exposes the current adversarial vulnerability of face-related systems.

Our main contributions can be summarized as follows:

- We first explore decision-based attacks on face forgery detection and verify their adversarial vulnerability.
- We propose cross-task perturbation initialization to handle initialization failures to attacks by leveraging the high correlation of face features across tasks without requiring any knowledge of detectors.
- Inspired by the frequency clues of face forgery detection, we propose a frequency decision-based attack that adds perturbations in the frequency domain and then constrains the visual quality in the spatial domain.
- Experiments show that our method achieves state-of-the-art attack performance on FaceForensics++, CelebDF, and industrial APIs, which exposes the vulnerability of face forgery detection under decision-based attacks.

The remainder of the paper is organized as follows. Section II briefly introduces face forgery detection and decision-based black-box attacks, and then discusses adversarial attacks on face forgery detection. Section III first gives the formal definition of decision-based attacks on face forgery detection. Then, we introduce Cross-task Perturbation Initialization and propose the Frequency Decision-based Attack. Section IV presents experiments to illustrate the effectiveness of the proposed method, including attacks on state-of-the-art detectors, ablation studies, attacks on industrial APIs, etc. We further discuss the possibility of using face-related tasks to assist in attacking face forgery detection in Section V and conclude this paper in Section VI.

## II. RELATED WORK

### A. Face Forgery Detection

Since large-scale public datasets are freely available, combined with rapid progress in generative models, a very realistic fake face has been generated with its corresponding implications for society. Therefore, there have been many efforts to distinguish real and fake faces as much as possible in face forgery detection. Early work [18] directly uses convolutional neural networks (CNNs) to extract discriminative features for face forgery detection. However, these spatial features extracted by CNNs focus more on class-level distinctions rather than subtle differences between real and fake faces. Furthermore, recent work [16], [17], [36] mines forgery patterns and proposes many frequency-based detection methods, noting that real and fake faces are diverse in the frequency domain. As a two-branch network, F<sup>3</sup>Net [16] finds forgery patterns using frequency clues and extracts discrepancies between real and fake images by looking at frequency statistics. Considering the potential of the recent Vision Transformer [4], M2TR [17] utilizes a multi-scale transformer for capturing local inconsistencies at different scales and additionally introduces frequency modality to improve performance with multiple image compression algorithms. To better evaluate the adversarial robustness of face forgery detection, we choose spatial-based [1]–[4] and frequency-based detectors [16], [17] for experiments.

### B. Decision-based Black-box Attacks

In contrast to white-box attacks that require access to model details such as architecture and gradients, recent work has focused on black-box attacks [29], including transfer-based, score-based, and decision-based attacks. Transfer-based attacks need to know the distribution of the data to construct the surrogate model and its performance is limited by the surrogate model. The difference between score-based and decision-based attacks is that the output returned by the threat model is a confidence or a label. It is obvious that the decision-based setting is the most difficult, but it is also the most practical since in reality, the adversary only knows minimal information about the model.

Brendel et al. [29] propose the first decision-based attack to randomly walk on the decision boundary starting from an

adversarial point while keeping adversarial, called the Boundary Attack. Some works [30]–[32], [34] improve Boundary Attack from the perspective of gradient optimization. Next, SignFlip [33] introduces noise projection and random sign flip to improve decision-based attack by large margins. RayS [35] reduces the number of queries by reformulating the continuous problem of finding the closest decision boundary into a discrete problem, which does not require zeroth-order gradient estimation. In this paper, we explore decision-based attacks on face forgery detection under  $l_\infty$  norm, i.e. adding perturbation within the perturbation range  $\epsilon$ , which is more practical in real-world applications.

### C. Adversarial Attacks on Face Forgery Detection

Face forgery detection is a security-sensitive task and its adversarial vulnerability has received much attention [20], [24]–[27]. Carlini et al. [20] and Neekhara et al. [25] shows the adversarial robustness of face forgery detectors under various white-box attacks and transfer-based attacks. Hussain et al. [37] evaluate the detectors by the score-based attack with natural evolutionary strategies [38]. Li et al. [26] manipulate the noise and latent vectors of StyleGAN [14] to fool face forgery detectors. KRA [24] attacks the key regions of forged faces obtained from the semantic region selection and boosts the adversarial transferability. Then, Jia et al. [27] add adversarial perturbations in the frequency domain and generate more imperceptible adversarial examples with a high transferability. In this paper, considering academic and industrial applications, we focus on attacking frame-level detectors because recent attacks on face forgery detection have mainly focused on attacking frame-level detectors [20], [24]–[27], and industrial APIs tend to use images as input because of the low computation and communication costs. In conclusion, we evaluate the adversarial robustness of face forgery detection under decision-based attacks for the first time and hope to provide insight into possible future improvements.

## III. METHODOLOGY

In this section, we first introduce preliminaries about decision-based attacks and the threat model. Then, we propose the cross-task perturbation initialization. Finally, we introduce the frequency perturbation into the decision-based attacks against face forgery detection.

### A. Preliminaries

We define a neural network-based face forgery detector  $f: \mathbb{R}^d \rightarrow \mathbb{R}^k$  as the threat model. Because the face forgery detection is a binary classification task, its label  $y$  is real or fake, i.e.  $y \in \mathbb{R}^2 = \{0, 1\}$ . Given a face  $x \in [0, 1]^d$ , we define  $f(x)_i$  as the probability of class  $i$  and  $c(x) = \operatorname{argmax}_{i \in \{0, 1\}} f(x)_i$  refers to the predicted label. In this paper, we only consider faces that are classified as fake and treat the situation where fake faces are classified as real faces as successful attacks. Therefore, the adversary aims to find an adversarial perturbation  $\delta \in \mathbb{R}^d$  such that  $c(x + \delta) = 0$  (classified as real). Here, we define  $\|\delta\|_\infty \leq \epsilon$  and  $\epsilon$  is the allowed maximum perturbation.

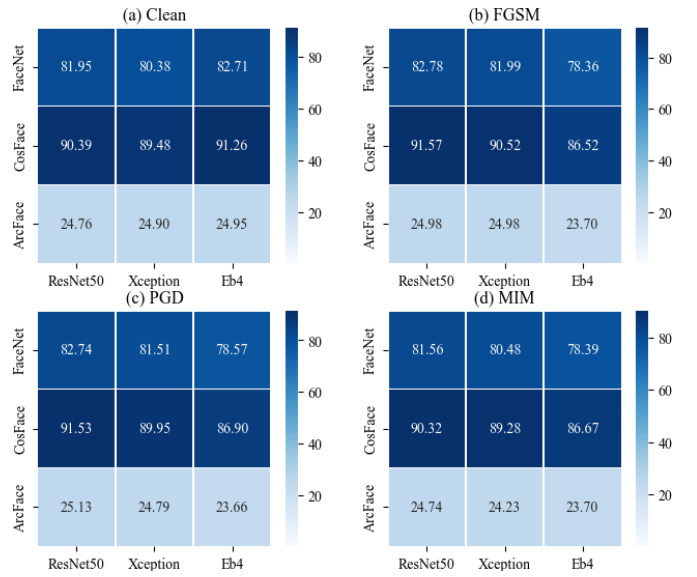


Fig. 2. Empirical analysis of cosine similarity (%) on intermediate features between forgery detectors and face recognition models under clean examples and adversarial examples (FGSM [22], PGD [39], and MIM [40]). We find that face recognition models and face forgery detectors have a high correlation between the intermediate features of the same face. It means that the perturbation of attacking face recognition can also perturb face forgery detection to a certain extent.

In the decision-based setting, the adversary does not have access to the model’s network architecture, weights, gradients, or the model’s predicted probabilities  $f(x)$ , only the model’s predicted labels  $c(x)$ . Therefore, the optimization objective of the decision-based attack is followed as:

$$\min_{\delta} \|\delta\|_\infty \quad \text{s.t.} \quad c(x + \delta) = 0. \quad (1)$$

The adversary keeps querying the model and optimizing adversarial perturbations  $\delta$  until  $\|\delta\|_\infty \leq \epsilon$ .

### B. Cross-task Perturbation Initialization

The easiest way to explore decision-based attacks in face forgery detection is to apply existing decision-based attacks directly [29]–[34]. In the case study, we choose the state-of-the-art HSJA [32], SignFlip [33], and RayS [35]. We apply these attacks directly to face forgery detection and find that they cause the attack to fail. Specifically, they all have a situation where the initialization fails, and the attack success rate is close to 0%. It shows that the random initialization is unsuccessful and cannot guarantee adversarial. Face forgery detection usually recognizes faces with random noises as fake faces because adding random noises is a common manipulation. Furthermore, using real faces as initialization can guarantee adversarial, but it may lead to artifacts, so image quality is not guaranteed. Hence, we hope a perturbation initialization can handle this issue while ensuring query efficiency.

Naturally, exploiting the adversarial transferability of face forgery detectors is a possible strategy. However, in practice, we not only do not have access to the training data of the threat model but also do not know the face forgery generation method it adopts, which greatly limits the possibility of using

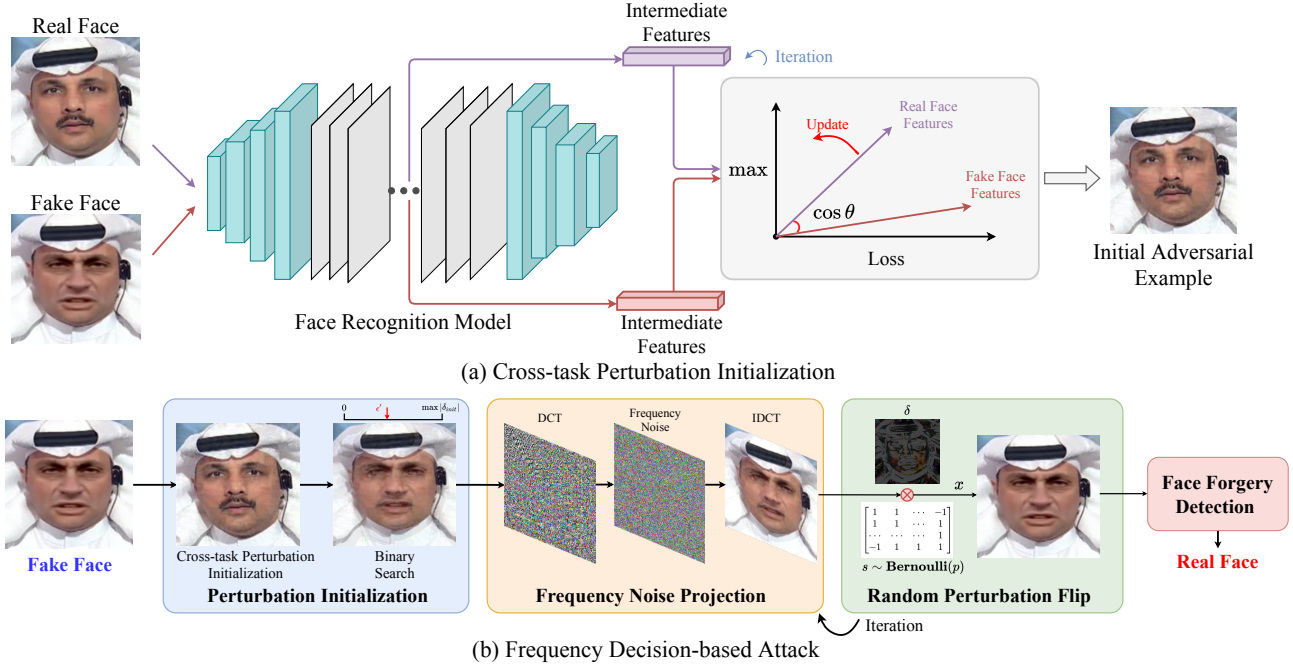


Fig. 3. (a) The overview of cross-task perturbation initialization. With the high correlation of intermediate features between face-related tasks, we iteratively update the real face, keeping it adversarial while improving efficiency for subsequent attacks. (b) The pipeline of the frequency decision-based attack. We first obtain the initial perturbation by perturbation initialization. Then, we iterate in frequency noise projection and random perturbation flip until  $c(x_{adv}) = 0$  and  $\|\delta\|_\infty \leq \epsilon$ .

---

#### Algorithm 1 Cross-task Perturbation Initialization

---

**Input:** Fake face  $x$ , real face  $x_r$ , face recognition model  $Z$   
**Parameters:** Maximum perturbation  $\xi$ , layer  $l$ , iteration number  $K$   
**Output:** Adversarial face  $x_{adv}$

- 1:  $x_0 \leftarrow x_r, \delta_0 \leftarrow 0$
- 2: **for**  $i \in [1, K]$  **do**
- 3:  $J(x_{i-1}, x) \leftarrow -\text{Cos}(Z_l(x_{i-1}), Z_l(x))$
- 4:  $\delta_i \leftarrow \delta_{i-1} + \frac{\xi}{K} \cdot \text{sign}(\nabla_{x_{i-1}} J(x_{i-1}, x))$
- 5:  $x_i \leftarrow \text{Clip}_{x_r, \xi}(x_{i-1} + \delta_i)$
- 6: **end for**
- 7:  $x_{adv} \leftarrow x_K$
- 8: **return**  $x_{adv}$

---

transfer adversarial perturbations. Since face recognition is a very common face-related task, it may help the attack achieve perturbation initialization. Furthermore, inspired by [41], intermediate features may have high correlations between different face-related tasks. From this perspective, using face recognition models to transfer adversarial perturbations is a feasible initialization strategy.

We assume that if there is a high degree of similarity between the intermediate features of the face recognition model and face forgery models, then attacking the face recognition model is equivalent to attacking the face forgery models. To verify the correlation of intermediate features across face tasks, we conduct an empirical study on FaceForensics++ [18]. We randomly select 256 frames to calculate the intermediate features and then average for calculating cosine similarity.

Fig. 2 shows the cosine similarity of intermediate features between face forgery detectors and face cognition models. The middle layer selection of the face recognition model is shown in Table V and the face forgery detectors select the second block unit. According to Fig. 2, we find that face recognition models and face forgery detectors have a high correlation between the intermediate features of the same face because these are all face-related tasks and models capture the general features of faces.

The above observations illustrate the high correlation of intermediate features between face-related tasks. Due to the high correlation between the intermediate features of face recognition and face forgery detection, the perturbation of attacking face recognition can also perturb face forgery detection to a certain extent, so we propose cross-task perturbation initialization. Given a face recognition model  $Z$ ,  $l$  represents the  $l$ -th layer, and  $Z_l(\cdot)$  represents the intermediate feature of the  $l$ -th layer. Considering attacking face forgery detectors, the adversary has a real face  $x_r$  and a forged fake face  $x$ . Usually,  $x_r$  is selected as the initialization to ensure adversarially, and then the distance from  $x$  is reduced. Therefore, the optimization objective for cross-task adversarial perturbation is as follows:

$$\underset{\delta}{\text{argmin}} \text{Cos}(Z_l(x), Z_l(x_r + \delta)), \quad s.t. \quad \|\delta\|_\infty \leq \xi, \quad (2)$$

where  $\xi$  is maximum cross-task perturbation and  $\text{Cos}$  calculates the cosine similarity between  $Z_l(x)$  and  $Z_l(x_r + \delta)$ . By minimizing the cosine similarity between  $Z_l(x)$  and  $Z_l(x_r + \delta)$ , we keep  $x_r + \delta$  away from fake faces  $x$  in the feature space

and move it towards real faces, thus providing a more correct attack direction and improve query efficiency.

Algorithm 1 illustrates the whole pipeline of the cross-task perturbation initialization, where  $\text{sign}$  represents the sign operation on the gradient and  $\text{Clip}_{x_r, \xi}(\cdot)$  projects the perturbation  $\delta$  to  $\xi$ -ball in order to satisfy  $\|\delta\|_\infty \leq \xi$ . The time complexity of CPI is  $O(K)$ , so the calculation of CPI requires  $K$  times of forward and backward propagation of the FR model. In this paper,  $K = 10$ . We test the time to calculate CPI on the A100, which is about 50.34ms for an image, with almost no additional overhead.

Compared with [41], we leverage the fast sign gradient to generate perturbations efficiently and focus on the high feature correlation between face-related tasks, which is beneficial to the generalizability of our method to adversarial attacks and defenses on more face-related tasks. Face recognition distinguishes the identities of different faces and enables the acquisition of more discriminative features. Therefore, CPI can provide a better initialization for face forgery detection, which ensures a more correct optimization direction and provides the possibility of attacking multiple face-related intelligent systems simultaneously.

### C. Frequency Decision-based Attack

Recent work [16], [17], [36] on face forgery detection has illustrated a significant difference in frequency between real and fake faces. In addition, some work [42]–[44] also shows that different models rely on different frequency components to make decisions. Inspired by these works, we consider adding noise directly to the frequency of human faces, *aiming to eliminate the difference between real and fake faces in frequency to improve the attack efficiency.*

Based on the general framework of decision-based attacks [32], [33], we propose the frequency decision-based attack (FDA) on face forgery detection. Fig. 3 summarizes the pipeline of our proposed attack, including the perturbation initialization, the frequency noise projection, and the random perturbation flip. Specifically, we first generate the cross-task adversarial perturbation  $\delta_{init}$  by perturbation initialization and resort to binary search to reduce the perturbation magnitude and guarantee adversarial. In frequency noise projection, we add perturbations in the frequency domain and constrain image quality in the spatial domain. Then, we randomly inverse the sign of the partial perturbation, expecting a better adversarial perturbation. Finally, we iterate in frequency noise projection and random perturbation flip until  $c(x_{adv}) = 0$  and  $\|\delta\|_\infty \leq \epsilon$ .

**Perturbation Initialization.** Generally speaking, the perturbation initialization is used in decision-based attacks to make clean examples keep adversarial. Given a face classified as real, we utilize the cross-task perturbation initialization to obtain initial perturbations  $\delta_{init}$ , which satisfies the adversarial constraint. Note that cross-task adversarial perturbations are imperceptible, so faces after cross-task perturbation initialization remain adversarial. Further, in order to reduce the magnitude of the initial perturbation, we choose to apply the binary search to make the initial adversarial face as close to  $x$  as possible. Binary search in perturbation initialization

---

### Algorithm 2 Binary Search

---

**Input:** Fake face  $x$ , initial perturbation  $\delta_{init}$

**Parameters:** iteration number  $k$

**Output:** Final initial perturbation  $\delta$

```

1:  $l \leftarrow 0, u \leftarrow \max(|\delta_{init}|)$ 
2: for  $i \in [1, k]$  do
3:    $m \leftarrow (l + u)/2$ 
4:    $x_t \leftarrow \text{Clip}_{x_r, m}(x + \delta_{init})$ 
5:   if  $c(x_t) = 0$  then
6:      $u \leftarrow m$ 
7:   else
8:      $l \leftarrow m$ 
9:   end if
10: end for
11:  $\delta \leftarrow \text{Clip}_{0, u}(\delta_{init})$ 
12: return  $\delta$ 

```

---

is summarized in Algorithm 2. Given an initial perturbation  $\delta_{init}$ , we continuously dichotomize the perturbation range from  $[0, \max(\delta_{init})]$  on the premise of ensuring adversarial, and finally obtain the final adversarial perturbation  $\delta$ . In this paper, we set  $k$  to 10. With the help of binary search, we obtain the final initial perturbation  $\delta$ , where  $\|\delta\|_\infty \leq \epsilon', \epsilon' \in (0, \max|\delta_{init}|]$ .

**Frequency Noise Projection.** Here,  $\mathcal{D}(\cdot)$  denotes discrete cosine transform (DCT) and  $\mathcal{D}'(\cdot)$  denotes inverse discrete cosine transform (IDCT). First, we transform the image from the spatial domain to the frequency domain with DCT. Then we add a random noise in the frequency domain  $\eta \sim \{-\gamma, \gamma\}^d$ . Finally, we project it to the  $\epsilon'$ -ball in the spatial domain and gradually decrease  $\epsilon'$  until it is satisfied  $\epsilon' \leq \epsilon$ . The specific calculation is as follows:

$$x_{idct} \leftarrow \mathcal{D}'(\mathcal{D}(x_{adv}) + \eta), \quad \eta \sim \{-\gamma, \gamma\}^d, \quad (3)$$

$$x_{adv} \leftarrow \text{Clip}_{x, \epsilon' - \kappa}(x_{idct}), \quad (4)$$

where  $\kappa$  is 0.004. For convenience, we perform DCT and IDCT on the whole image. Note that  $x$  and  $\mathcal{D}'(\mathcal{D}(x))$  are equivalent. However, after adding the noise  $\eta$  to  $\mathcal{D}(x)$  on the frequency domain,  $x$  and  $\mathcal{D}'(\mathcal{D}(x) + \eta)$  are not equivalent.  $\eta$  is transformed into a frequency domain distribution with the help of frequency information according to IDCT.

**Random Perturbation Flip.** Existing work [45], [46] shows that searching on the nodes of the  $l_\infty$  ball is more efficient than searching in the  $l_\infty$  ball. Motivated by these observations, both [33] and [35] suggest some strategies based on searching on the  $l_\infty$  ball. Here, we choose [33] to further accelerate the attack. After the frequency noise projection, we randomly partial coordinates to flip the signs of perturbation. Suppose  $s \in \{-1, 1\}^d$  and  $p \in (0, 1)^d$ , the random perturbation flip is formulated by:

$$s \sim \text{Bernoulli}(p), \quad \delta_s \leftarrow \delta_p \odot s. \quad (5)$$

The frequency decision-based attack is shown in Algorithm 3. Based on the cross-task perturbation initialization, the frequency decision-based attack can threaten face forgery detection and better ensure the image quality, which is convenient for the application of downstream tasks.

**Algorithm 3** Frequency Decision-based Attack

**Input:** Fake face  $x$ , real face  $x_r$ , face recognition model  $Z$ , face forgery detector  $f$

**Parameters:** Maximum perturbation  $\epsilon$ , step size  $\gamma$

**Output:** Adversarial face  $x_{adv}$

---

```

1: # Perturbation Initialization
2:  $\delta_{init} \leftarrow \text{CrossPerturbInit}(x, x_r, Z, f)$ 
3:  $\delta \leftarrow \text{BinarySearch}(x, \delta_{init})$ 
4:  $\epsilon' \leftarrow \|\delta\|_\infty$ 
5: while  $\epsilon < \epsilon'$  do
6:    $x_{dct}^p \leftarrow \mathcal{D}(x + \delta)$  # Frequency Noise Projection
7:    $\eta \sim \{-\gamma, \gamma\}^d$ 
8:    $x_{idct}^p \leftarrow \mathcal{D}'(x_{dct}^p + \eta)$ 
9:    $x^p \leftarrow \text{Clip}_{x, \epsilon' - \kappa}(x_{idct}^p)$ 
10:  if  $c(x^p) = 0$  then
11:     $\delta \leftarrow x^p - x$ 
12:  end if
13:   $s \sim \text{Bernoulli}(p)$  # Perturbation Random Flip
14:   $\delta^p \leftarrow \delta \odot s$ 
15:  if  $c(x + \delta^p) == 0$  then
16:     $\delta \leftarrow \delta^p$ 
17:  end if
18:   $\epsilon' \leftarrow \|\delta\|_\infty$ 
19: end while
20:  $x_{adv} \leftarrow x + \delta$ 
21: return  $x_{adv}$ 

```

---

## IV. EXPERIMENTS

In this section, we verify the effectiveness of the proposed method. First, we introduce the relevant settings of the experiments. We then provide experimental results on state-of-the-art detectors to illustrate the performance of our attack. Next, we conduct the ablation study to evaluate the effectiveness of the proposed module. Further, we evaluate the image quality of the generated adversarial examples. Finally, we further demonstrate the effectiveness of our method on industrial APIs, adversarial transferability, and adversarial defenses.

## A. Experimental Setup

**Datasets.** FaceForensics++ (FFDF) [18] is a popular large-scale face forgery dataset containing 1,000 video sequences. It includes four forging methods, Face2Face [10], FaceSwap [11], DeepFakes [12] and NeuralTextures [13]. We randomly select 4 frames of each video in the test set, a total of 560 frames (140×4=560). CelebDF [19] is a large-scale DeepFake video dataset with a total of 5,639 DeepFake videos. We also randomly select 500 frames from different videos from the testset.

**Models.** Face forgery detection is based on the spatial domain or frequency domain. For spatial-based face forgery detection, we choose four spatial-based classification networks, such as ResNet50 [1], Xception [2], EfficientNet-b4 (Eb4) [3] and ViT-B (ViT) [4]. For frequency-based face forgery detection, we choose state-of-the-art models, such as F<sup>3</sup>Net [16] and M2TR [17]. All the models are trained according to the corresponding paper settings. The accuracy

TABLE I  
THE ACCURACY OF SPATIAL-BASED AND FREQUENCY-BASED FACE FORGERY DETECTORS ON THE CELEBDF AND FFDF DATASETS.

Model	ResNet50	Xception	Eb4	ViT	F <sup>3</sup> Net	M2TR
CelebDF	98.51	99.05	99.44	96.73	96.47	99.76
FFDF	94.87	95.24	95.61	93.45	97.52	97.93

of these face forgery detectors is shown in Table I. For face recognition models, we choose FaceNet [47] to initialize cross-task perturbations.

**Attack Methods.** We compare the proposed algorithm with state-of-the-art attack algorithms, including Boundary Attack [29], Opt-Attack [30], Sign-Opt [31], Triangle Attack (TA) [34], HSJA [32], SignFlip [33], and RayS [35]. Attack parameters are consistent with corresponding attacks.

**Evaluation metrics.** We choose three metrics to quantitatively evaluate the performance of attack methods: attack success rate (ASR), average queries (AQ), and median queries (MQ). Attack success rate (ASR) is defined as the proportion of faces that are successfully attacked. Here, a successful attack is to classify fake faces as real faces. Average queries (AQ) and median queries (MQ) are only calculated over successful attacks, following [33] and [35].

**Implementation details.** We use Retinaface [48] to detect and crop faces and follow the open-source PyDeepFakeDet<sup>1</sup> for preprocessing. For the cropped face, the model resizes it to an image shape and then uses it as the model’s input. For decision-based attacks, we set the maximum perturbation of each pixel to be  $\epsilon = 0.05$  and the maximum query budget is 10,000. Since these attacks are initialized with randomness, it is easy to cause the attack to fail, so we choose to use the same real face as the initialization if the attack allows. For cross-task perturbation initialization, the cosine similarity of intermediate layer features is interpolated to the same dimension. Here,  $K = 10$ ,  $\gamma = 1.75$ ,  $\xi = 0.031$ , and  $p = 0.999$ . In the frequency decision-based attack, the attack ends when  $\epsilon \geq \epsilon'$  or the query reaches the maximum number of queries.

## B. Attacks on State-of-the-art Detectors

**Attack on Spatial-based Models.** Table II shows the attack success rates against spatial-based models on FaceForensics++ and CelebDF. Compared with other attacks, our method has a higher query efficiency on the premise of ensuring 100% attack success rate. Furthermore, Boundary, SignFlip, and RayS fail to attack some models (e.g. ResNet50, Eb4) even with real faces as perturbation initialization. For example, SignFlip and RayS attack Eb4 fails on FaceForensics++, but our method achieves the attack with a high attack efficiency. Meanwhile, compared to SignFlip and RayS, the average query number of our method is 1/2 and 1/7 of that on ResNet50, and 1/5 and 1/160 of that on Xception. On CelebDF, our method improves the attack efficiency by 17.90% and 23.81% against Xception and Eb4 compared to the state-of-the-art SignFlip.

<sup>1</sup><https://github.com/wangjik666/PyDeepFakeDet/blob/main/DATASET.md>

TABLE II  
ATTACK RESULTS OF DECISION-BASED ATTACKS AGAINST SPATIAL-BASED FACE FORGERY DETECTION ON FACEFORENSICS++ AND CELEBDF.

Dataset	Model	ResNet50			Xception			Eb4			ViT		
		Method	AQ↓	MQ↓	ASR(%)↑	AQ↓	MQ↓	ASR(%)↑	AQ↓	MQ↓	ASR(%)↑	AQ↓	MQ↓
FFDF	Boundary	6607.10	6363.0	5.50	5165.22	4819.0	15.20	-	-	0.00	3679.73	3473.0	8.04
	Opt	5105.91	4883.0	65.17	4490.10	4204.0	82.14	4826.47	4394.0	69.11	3393.52	3482.0	30.00
	SignOpt	1780.87	1552.0	5.54	4113.86	3328.0	20.11	1342.23	831.0	11.07	1342.22	831.0	11.17
	TA	1000.00	1000.0	37.68	1000.00	1000.0	46.96	1000.00	1000.0	25.71	1000.00	1000.0	80.35
	HSJA	198.02	190.0	<b>100.00</b>	186.55	186.0	<b>100.00</b>	246.25	191.0	96.25	245.19	188.0	79.64
	SignFlip	53.51	50.0	<b>100.00</b>	63.93	50.0	<b>100.00</b>	-	-	0.00	167.85	78.0	99.28
	RayS	152.84	133.0	<b>100.00</b>	1965.08	1580.0	<b>100.00</b>	-	-	0.00	312.35	270.0	<b>100.00</b>
	Ours	<b>21.70</b>	<b>12.0</b>	<b>100.00</b>	<b>12.72</b>	<b>12.0</b>	<b>100.00</b>	<b>39.94</b>	<b>34.0</b>	<b>96.96</b>	<b>139.86</b>	<b>42.0</b>	<b>100.00</b>
CelebDF	Boundary	-	-	0.00	4159.81	3594.0	10.40	4438.24	3349.0	5.00	5586.00	5460.0	0.60
	Opt	6939.37	7374.0	20.40	2101.52	1340.0	96.00	3925.10	3354.0	87.60	5800.34	6031.0	18.60
	SignOpt	3541.41	3124.0	37.80	1260.02	926.0	73.00	1752.79	1737.0	60.8	3282.36	2873.0	25.00
	TA	1000.00	1000.0	92.20	1000.00	1000.0	86.00	1000.00	1000.0	96.8	1000.00	1000.0	78.00
	HSJA	232.74	189.0	70.00	187.11	186.0	99.20	188.24	188.0	<b>100.00</b>	1595.12	327.0	18.00
	SignFlip	33.39	<b>12.0</b>	99.60	15.25	<b>12.0</b>	99.20	20.32	<b>12.0</b>	<b>100.00</b>	288.99	98.0	99.60
	RayS	-	-	0.00	203.16	175.0	<b>100.00</b>	169.85	140.0	<b>100.00</b>	<b>237.76</b>	215.0	<b>100.00</b>
	Ours	<b>32.98</b>	<b>12.0</b>	<b>100.00</b>	<b>12.52</b>	<b>12.0</b>	<b>100.00</b>	<b>15.48</b>	<b>12.0</b>	<b>100.00</b>	283.34	<b>92.0</b>	<b>100.00</b>

TABLE III  
ATTACK RESULTS OF DECISION-BASED ATTACKS AGAINST FREQUENCY-BASED DETECTORS ON FACEFORENSICS++ AND CELEBDF.

Dataset	Model	F <sup>3</sup> Net			M2TR		
		Method	AQ↓	MQ↓	ASR(%)↑	AQ↓	MQ↓
FFDF	Boundary	3313.41	2456.0	12.06	2202.50	1427.0	3.04
	Opt	3435.38	3286.0	5.53	3549.99	3029.0	79.46
	SignOpt	4262.19	3956.0	19.56	1078.89	785.0	45.90
	TA	1000.00	1000.0	33.21	1000.00	1000.0	77.14
	HSJA	199.38	187.0	82.50	886.46	188.0	81.42
	SignFlip	732.11	280.0	93.57	102.07	86.0	<b>100.00</b>
	RayS	<b>140.30</b>	117.0	99.92	225.33	157.0	<b>100.00</b>
	Ours	152.25	<b>114.0</b>	<b>100.00</b>	<b>79.19</b>	<b>60.0</b>	<b>100.00</b>
CelebDF	Boundary	3393.24	2883.0	22.00	1920.33	14.0	1.80
	Opt	1839.61	1178.0	95.60	5053.90	5363.0	30.60
	SignOpt	1220.62	868.0	59.20	2752.79	2549.0	71.20
	TA	1000.00	1000.0	89.20	1000.00	1000.0	90.00
	HSJA	187.04	186.0	<b>100.00</b>	1275.91	324.0	33.60
	SignFlip	19.54	<b>12.0</b>	97.20	103.84	<b>12.0</b>	<b>100.00</b>
	RayS	84.54	77.0	<b>100.00</b>	84.21	79.0	<b>100.00</b>
	Ours	<b>12.59</b>	<b>12.0</b>	<b>100.00</b>	<b>32.67</b>	<b>12.0</b>	<b>100.00</b>

TABLE IV  
ABLATION STUDY ON KEY MODULES. FREQUENCY NOISES AND CROSS-TASK PERTURBATION INITIALIZATION SIGNIFICANTLY IMPROVE THE ATTACK EFFICIENCY, ILLUSTRATING ITS EFFECTIVENESS.

Fre_Noise	CPI	ResNet50			ViT		
		AQ↓	MQ↓	ASR(%)↑	AQ↓	MQ↓	ASR(%)↑
		57.79	48.0	100.00	167.99	72.0	99.21
✓		53.95	44.0	100.00	164.23	66.0	100.00
	✓	27.25	16.0	100.00	160.04	62.0	100.00
✓	✓	<b>23.75</b>	<b>14.0</b>	100.00	<b>158.42</b>	<b>56.0</b>	100.00

Although less related to the features of ViT, our method can also achieve a state-of-the-art attack success rate, which effectively illustrates the generalization of our method.

**Attack on Frequency-based Models.** Face forgery detection often uses the difference in frequency as a clue to judge

TABLE V  
THE SELECTION OF INTERMEDIATE FEATURE LAYERS OF FACE RECOGNITION MODELS. THE **BOLDED INTERMEDIATE FEATURE LAYERS** ARE USED TO IMPLEMENT CROSS-TASK PERTURBATION INITIALIZATION.

Model	Layer1	Layer2	Layer3	Layer4
FaceNet	conv2d_2b	<b>conv2d_4b</b>	mixed_7a	block8
CosFace	layer1	layer2	<b>layer3</b>	layer4
ArcFace	layer1	<b>layer2</b>	layer3	layer4

whether it is forgery. To verify the adversarial robustness of these frequency-based methods, we choose F<sup>3</sup>Net [16] and M2TR [17] for experiments. Table III shows the attack success rates of frequency-based detectors on FaceForensics++ and CelebDF. Frequency-based detectors perform well on face forgery detection, but they are just as susceptible to adversarial robustness as spatial-based detectors. On F<sup>3</sup>Net, our method achieves state-of-the-art attack performance, especially on CelebDF, with 35.56% fewer queries on average than SignFlip. On M2TR, our method improves the query efficiency by 22.41% and 61.20% over state-of-the-art methods on FaceForensics++ and CelebDF, respectively. Experiments demonstrate the effectiveness of our method in frequency-based detectors, and further expose the adversarial vulnerability of face forgery detection.

### C. Ablation Study

In this section, we choose ResNet50 [1] and ViT [4] as the threat models and randomly select 128 faces ( $4 \times 32 = 128$ ) on FaceForensics++ [18] for the ablation study.

**Key Modules.** We first investigate the impact of the proposed key modules on the attack efficiency. Fre\_Noise represents whether to add noises in the frequency domain (refer to Eq. 3), and CPI represents cross-task perturbation initialization. As shown in Table IV, adding frequency noises or cross-task perturbation initialization individually brings

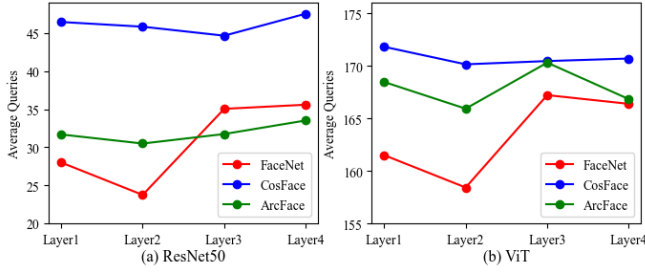


Fig. 4. Ablation study on intermediate feature layers. We find that middle-layer features tend to have better attack performance. In addition, FaceNet has a better initialization effect than CPI’s face recognition model.

TABLE VI  
ABLATION STUDY ON THE FREQUENCY NOISE MAGNITUDE  $\gamma$ .

$\gamma$	ResNet50			ViT		
	AQ↓	MQ↓	ASR(%) <sup>↑</sup>	AQ↓	MQ↓	ASR(%) <sup>↑</sup>
2.5	23.00	14.00	100.00	171.29	42.00	100.00
2.0	23.89	14.00	100.00	163.09	42.00	100.00
1.75	<b>23.75</b>	14.00	100.00	<b>158.42</b>	42.00	100.00
1.5	24.34	14.00	100.00	<b>158.42</b>	46.00	100.00
1.0	26.15	14.00	100.00	152.63	54.00	100.00

gains (i.e., 6.65%/52.84% on ResNet50, 2.23%/4.73% on ViT), revealing the effectiveness of the corresponding key modules. Combing all modules together leads to the best attack performance, yielding the query efficiency of 58.90% and 5.69% on ResNet50 and ViT, respectively.

**Intermediate Feature Layers.** We choose different face recognition models (FaceNet [47], CosFace [49], and ArcFace [50]) and consider choosing different intermediate feature layers to craft cross-task adversarial perturbations. Table V illustrates the selection of intermediate feature layers, and Fig. 4 illustrates the average number of queries for different intermediate feature layers. Attacking the features of the middle layer achieves better results than attacking the top or bottom layers, so we choose to use the bold layers in Table V to generate cross-task adversarial perturbations. Besides, FaceNet has better attack efficiency than other models, so we choose FaceNet as the face recognition model initialized by cross-task perturbation.

**Frequency noise magnitude  $\gamma$ .** The magnitude of the frequency perturbation is critical to the efficiency of the attack. Table VI illustrates the effect of different frequency noise magnitudes  $\gamma$  on the attack efficiency. When the  $\gamma$  is 1.75, ResNet50 and ViT achieve the smallest AQ and MQ, and maintain a 100% attack success rate. Therefore, the  $\gamma$  in this paper is 1.75.

#### D. Image Quality Assessment

In this section, we analyze the image quality assessment of adversarial examples generated on FaceForensics++ [18]. Due to page limitations, here we choose Xception as the threat model, and state-of-the-art Signflip [33] and RayS [35] for comparison. To assess the image quality, MSE, PSNR, and

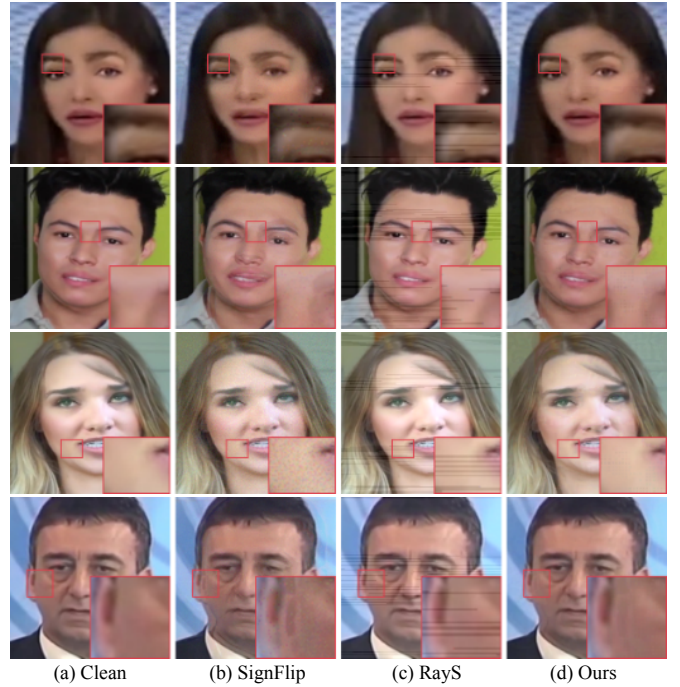


Fig. 5. Visual qualitative evaluation on SignFlip, RayS, and ours on FaceForensics++. From top to bottom, the forged faces are from Deepfake, Face2Face, FaceSwap, and NeuralTextures.

SSIM [51] are used as evaluation metrics to quantify the difference between adversarial and real faces. As shown in Table VII, our method outperforms other attacks by a wide margin in terms of MSE, PSNR, and SSIM. Further, we visualize the adversarial examples generated by SignFlip, RayS, and our method in Fig. 5. The adversarial examples generated by our method are more imperceptible, unlike SignFlip with artifacts or RayS with obvious black lines. Finally, to verify that better image quality can attack both face recognition and face forgery detection, we choose the recognition success rate (RSR, %) as the evaluation criterion. We compare the face of adversarial examples in Table II with the real face of its same identity, and the results are shown in Table VII. In addition, frequency noise significantly improves image quality. It shows that our method has stronger attack performance while maintaining high image quality since our method is able to break both face recognition and face forgery detection.

#### E. Attacks on industrial APIs

In this section, we investigate the applicability of decision-based attacks on real-world systems, such as commercial face forgery detection APIs. We regard the face forgery detection API<sup>2</sup> on Tencent AI Open Platform as the threat model. We choose the detection threshold to be 0.5, that is, if the output is greater than the threshold, the input is judged as fake faces. Simultaneously, we choose the face recognition API<sup>3</sup> on Tencent AI Open Platform to calculate the recognition success rate (RSR, %). For face comparison, we choose a

<sup>2</sup><https://cloud.tencent.com/product/atdf?fromSource=gwzcgw>

<sup>3</sup><https://ai.qq.com/product/face.shtml#compare>

TABLE VII  
QUANTITATIVE IMAGE QUALITY ASSESSMENT OF ADVERSARIAL  
EXAMPLES GENERATED BY SIGNFLIP [33], RAYS [35], AND OUR  
METHOD ON FACEFORENSICS++ [18].

Attack	MSE↓	PSNR↑	SSIM↑	RSR(%)↑
Clean	-	-	-	<b>73.75</b>
SignFlip	127.4	27.40	0.8525	72.67
RayS	81.4	29.54	0.7630	71.96
Ours w.o. Fre_Noise	74.4	30.11	0.8195	73.21
Ours	<b>42.7</b>	<b>32.63</b>	<b>0.8766</b>	73.39

TABLE VIII  
EXPERIMENTAL RESULTS FOR ATTACKING INDUSTRIAL APIS.

Attack	$\epsilon = 0.062$				$\epsilon = 0.125$			
	AQ↓	MQ↓	ASR(%)↑	RSR(%)↑	AQ↓	MQ↓	ASR(%)↑	RSR(%)↑
SignFlip	92.80	<b>12.0</b>	40.00	21.00	39.51	<b>12.0</b>	74.00	24.00
RayS	-	-	0.00	0.00	-	-	0.00	0.00
Ours	<b>80.18</b>	<b>12.0</b>	<b>66.00</b>	<b>38.00</b>	<b>38.18</b>	<b>12.0</b>	<b>75.00</b>	<b>27.00</b>

similarity threshold of 60. We choose 100 random frames of FaceForensics++ [18] as test samples, including four forging methods, Face2Face [10], FaceSwap [11], DeepFakes [12] and NeuralTextures [13].

Here, we set the maximum number of queries to 1,000 and the maximum perturbation  $\epsilon$  to 0.062 and 0.125. RSR is only calculated on successful samples identified as real faces. Table VIII shows the experimental results of attacking industrial APIs, and Figure 6 shows the visualization of attacking commercial APIs. Note that RayS [35] is ineffective in attacking industrial APIs. This is because RayS’ perturbation initialization causes the image to become black, making the API unable to detect faces, and eventually leading to API denial of service. Compared with SignFlip [33], our method has a higher attack success rate (26% ↑ and 1% ↑) and lower query efficiency under different  $\epsilon$ . In terms of recognition success rate (RSR), our method outperforms the baseline with an improvement of 17.00% and 3.00%, respectively, which can be attributed to the better image quality produced by our method. This suggests that our method is more effective in simultaneously attacking face recognition and face forgery detection systems. Therefore, our method can effectively evaluate the security of existing AI systems in real-world scenarios.

#### F. Adversarial Transferability

In this section, we evaluate the cross-dataset adversarial transferability of different decision-based attacks. We generate adversarial examples on CelebDF [19] and then test the same model on FFDF [18]. Table IX shows that the attack success rate (%) on cross-dataset evaluation. Because our method can eliminate the difference between real and fake faces in the frequency domain, it has stronger cross-dataset adversarial transferability.

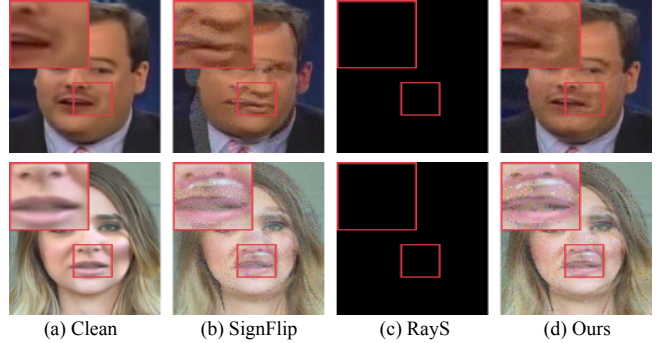


Fig. 6. Visualization of generated adversarial examples for attacking commercial APIs ( $\epsilon = 0.125$ ). RayS is denied access because the perturbation initialization fails to detect faces. Compared with SignFlip, our method has a higher recognition success rate and can better attack both face recognition and face forgery detection.

TABLE IX  
CROSS-DATASET EVALUATION ON ADVERSARIAL TRANSFERABILITY.

Attack	Clean	SignFlip	RayS	Ours
ResNet50	8.8	50.8	-	<b>59.6</b>
ViT	17.8	80.4	54.2	<b>81.0</b>

#### G. JPEG Defense

JPEG [52] is a lossy image compression method designed to preferentially preserve details important to the human visual system, and therefore has become a mainstream adversarial defense method. To further evaluate the robustness of our method, we evaluate JPEG defenses in the form of adaptive attacks [52]. As shown in Table X, since JPEG [52] removes high-frequency features, our FDA adds noise at both high and low frequencies, thus marginally reducing attack efficiency but keeping 100% ASR because high-frequency noise is still effective.

## V. DISCUSSION

In this section, we further analyze the activation relationship of Cross-task Perturbation Initialization in face recognition and face forgery detection features in Section III-B. Face recognition distinguishes the identities of different faces. Recent work [53], [54] focuses on using face identities to enhance face forgery detection. The middle layer features of face recognition are positively correlated with face forgery detection, so the adversarial examples of face recognition can be used to attack face forgery detection, and we propose Cross-task Perturbation Initialization. Our work is the first to simultaneously attack two face-related tasks, face forgery detection and face recognition, in academic and industrial scenarios. Cross-task Perturbation Initialization on face recognition is also beneficial to attack face recognition and face forgery detection. Therefore, the introduction of face recognition may be the future research direction of face forgery detection.

## VI. CONCLUSIONS

In this paper, we first explore decision-based attacks on face forgery detection. The direct application of existing decision-based attacks, however, suffers from initialization failures and

TABLE X  
ATTACK PERFORMANCE WITH THE JPEG DEFENSE ON FFDF.

Method	AQ↓	MQ↓	ASR(%)↑
Ours	21.70	12.0	100.00
Ours+JPEG	36.88	26.0	100.00

low image quality. To alleviate initialization sensitivity on attacks, we propose cross-task perturbation that utilizes the high correlation of face features across tasks. Based on the frequency cues utilized in face forgery detection, we propose a frequency decision-based attack. In particular, we perturb the frequency domain and then constrain the visual quality in the spatial domain. Our method achieves high query efficiency and guaranteed image quality for FaceForensics++, CelebDF, and APIs, demonstrating state-of-the-art attack performance.

**Broader impacts.** The method proposed in this paper may threaten face-related applications to some extent, such as face recognition and face forgery detection. Further, through attacks, the method can mine the security vulnerabilities of existing applications, which is beneficial to the development of more secure applications in the future.

## REFERENCES

- [1] K. He, X. Zhang, S. Ren, and J. Sun, "Deep residual learning for image recognition," in *CVPR*, 2016, pp. 770–778.
- [2] F. Chollet, "Xception: Deep learning with depthwise separable convolutions," in *CVPR*, 2017, pp. 1800–1807.
- [3] M. Tan and Q. V. Le, "Efficientnet: Rethinking model scaling for convolutional neural networks," in *ICML*, vol. 97, 2019, pp. 6105–6114.
- [4] A. Dosovitskiy, L. Beyer, A. Kolesnikov, D. Weissenborn, X. Zhai, T. Unterthiner, M. Dehghani, M. Minderer, G. Heigold, S. Gelly, J. Uszkoreit, and N. Houlsby, "An image is worth 16x16 words: Transformers for image recognition at scale," in *ICLR*, 2021.
- [5] Z. Chen, B. Li, J. Xu, S. Wu, S. Ding, and W. Zhang, "Towards practical certifiable patch defense with vision transformer," in *CVPR*, 2022, pp. 15 148–15 158.
- [6] I. J. Goodfellow, J. Pouget-Abadie, M. Mirza, B. Xu, D. Warde-Farley, S. Ozair, A. C. Courville, and Y. Bengio, "Generative adversarial nets," in *NeurIPS*, 2014, pp. 2672–2680.
- [7] J. Song, C. Meng, and S. Ermon, "Denosing diffusion implicit models," in *ICLR*. OpenReview.net, 2021.
- [8] P. Dhariwal and A. Q. Nichol, "Diffusion models beat gans on image synthesis," in *NeurIPS*, M. Ranzato, A. Beygelzimer, Y. N. Dauphin, P. Liang, and J. W. Vaughan, Eds., 2021, pp. 8780–8794.
- [9] R. Rombach, A. Blattmann, D. Lorenz, P. Esser, and B. Ommer, "High-resolution image synthesis with latent diffusion models," in *CVPR*, 2022, pp. 10 674–10 685.
- [10] J. Thies, M. Zollhöfer, M. Stamminger, C. Theobalt, and M. Nießner, "Face2face: Real-time face capture and reenactment of RGB videos," in *CVPR*, 2016, pp. 2387–2395.
- [11] M. Kowalski, "Faceswap," 2018, <https://github.com/MarekKowalski/FaceSwap/>.
- [12] M. Tora, "Deepfakes," 2018, <https://github.com/deep-fakes/faceswap/tree/v2.0.0>.
- [13] J. Thies, M. Zollhöfer, and M. Nießner, "Deferred neural rendering: image synthesis using neural textures," *ACM TOG*, vol. 38, no. 4, pp. 66:1–66:12, 2019.
- [14] T. Karras, S. Laine, and T. Aila, "A style-based generator architecture for generative adversarial networks," *IEEE Trans. Pattern Anal. Mach. Intell.*, vol. 43, no. 12, pp. 4217–4228, 2021.
- [15] Z. Sun, S. Chen, T. Yao, B. Yin, R. Yi, S. Ding, and L. Ma, "Contrastive pseudo learning for open-world deepfake attribution," in *ICCV*, 2023, pp. 20 882–20 892.
- [16] Y. Qian, G. Yin, L. Sheng, Z. Chen, and J. Shao, "Thinking in frequency: Face forgery detection by mining frequency-aware clues," in *ECCV*, vol. 12357. Springer, 2020, pp. 86–103.
- [17] J. Wang, Z. Wu, W. Ouyang, X. Han, J. Chen, Y. Jiang, and S. Li, "M2TR: multi-modal multi-scale transformers for deepfake detection," in *ICMR*, 2022, pp. 615–623.
- [18] A. Rössler, D. Cozzolino, L. Verdoliva, C. Riess, J. Thies, and M. Nießner, "Faceforensics++: Learning to detect manipulated facial images," in *ICCV*, 2019, pp. 1–11.
- [19] Y. Li, X. Yang, P. Sun, H. Qi, and S. Lyu, "Celeb-df: A large-scale challenging dataset for deepfake forensics," in *CVPR*, 2020, pp. 3204–3213.
- [20] N. Carlini and H. Farid, "Evading deepfake-image detectors with white-and black-box attacks," in *CVPRW*, 2020, pp. 2804–2813.
- [21] Z. Chen, B. Li, S. Wu, J. Xu, S. Ding, and W. Zhang, "Shape matters: deformable patch attack," in *ECCV*. Springer, 2022, pp. 529–548.
- [22] I. J. Goodfellow, J. Shlens, and C. Szegedy, "Explaining and harnessing adversarial examples," in *ICLR*, 2015.
- [23] Z. Chen, B. Li, S. Wu, S. Ding, and W. Zhang, "Query-efficient decision-based black-box patch attack," *IEEE Trans. Inf. Forensics Secur.*, vol. 18, pp. 5522–5536, 2023.
- [24] Q. Liao, Y. Li, X. Wang, B. Kong, B. Zhu, S. Lyu, Y. Yin, Q. Song, and X. Wu, "Imperceptible adversarial examples for fake image detection," in *ICIP*, 2021, pp. 3912–3916.
- [25] P. Neekhara, B. Dolhansky, J. Bitton, and C. Canton-Ferrer, "Adversarial threats to deepfake detection: A practical perspective," in *CVPRW*, 2021, pp. 923–932.
- [26] D. Li, W. Wang, H. Fan, and J. Dong, "Exploring adversarial fake images on face manifold," in *CVPR*, 2021, pp. 5789–5798.
- [27] S. Jia, C. Ma, T. Yao, B. Yin, S. Ding, and X. Yang, "Exploring frequency adversarial attacks for face forgery detection," in *CVPR*, 2022, pp. 4093–4102.
- [28] H. Huang, Y. Wang, Z. Chen, Y. Zhang, Y. Li, Z. Tang, W. Chu, J. Chen, W. Lin, and K.-K. Ma, "Cmua-watermark: A cross-model universal adversarial watermark for combating deepfakes," in *AAAI*, vol. 36, no. 1, 2022, pp. 989–997.
- [29] W. Brendel, J. Rauber, and M. Bethge, "Decision-based adversarial attacks: Reliable attacks against black-box machine learning models," in *ICLR*, 2018.
- [30] M. Cheng, T. Le, P. Chen, H. Zhang, J. Yi, and C. Hsieh, "Query-efficient hard-label black-box attack: An optimization-based approach," in *ICLR*, 2019.
- [31] M. Cheng, S. Singh, P. H. Chen, P. Chen, S. Liu, and C. Hsieh, "Signopt: A query-efficient hard-label adversarial attack," in *ICLR*, 2020.
- [32] J. Chen, M. I. Jordan, and M. J. Wainwright, "Hopskipjumpattack: A query-efficient decision-based attack," in *IEEE Symp. Secur. and Priv.*, 2020, pp. 1277–1294.
- [33] W. Chen, Z. Zhang, X. Hu, and B. Wu, "Boosting decision-based black-box adversarial attacks with random sign flip," in *ECCV*, vol. 12360. Springer, 2020, pp. 276–293.
- [34] X. Wang, Z. Zhang, K. Tong, D. Gong, K. He, Z. Li, and W. Liu, "Triangle attack: A query-efficient decision-based adversarial attack," in *ECCV*, vol. 13665, 2022, pp. 156–174.
- [35] J. Chen and Q. Gu, "Rays: A ray searching method for hard-label adversarial attack," in *SIGKDD*, 2020, pp. 1739–1747.
- [36] J. Frank, T. Eisenhofer, L. Schönherr, A. Fischer, D. Kolossa, and T. Holz, "Leveraging frequency analysis for deep fake image recognition," in *ICML*, vol. 119, 2020, pp. 3247–3258.
- [37] S. Hussain, P. Neekhara, M. Jere, F. Koushanfar, and J. J. McAuley, "Adversarial deepfakes: Evaluating vulnerability of deepfake detectors to adversarial examples," in *IEEE Winter Conference on Applications of Computer Vision, WACV 2021, Waikoloa, HI, USA, January 3-8, 2021*. IEEE, 2021, pp. 3347–3356.
- [38] A. Ilyas, L. Engstrom, A. Athalye, and J. Lin, "Black-box adversarial attacks with limited queries and information," in *ICML*, vol. 80, 2018, pp. 2142–2151.
- [39] A. Madry, A. Makelov, L. Schmidt, D. Tsipras, and A. Vladu, "Towards deep learning models resistant to adversarial attacks," in *ICLR*, 2018.
- [40] Y. Dong, F. Liao, T. Pang, H. Su, J. Zhu, X. Hu, and J. Li, "Boosting adversarial attacks with momentum," in *CVPR*, 2018, pp. 9185–9193.
- [41] Z. Wei, J. Chen, Z. Wu, and Y. Jiang, "Cross-modal transferable adversarial attacks from images to videos," in *CVPR*, 2022, pp. 15 044–15 053.
- [42] H. Wang, X. Wu, Z. Huang, and E. P. Xing, "High-frequency component helps explain the generalization of convolutional neural networks," in *CVPR*, 2020, pp. 8681–8691.
- [43] D. Yin, R. G. Lopes, J. Shlens, E. D. Cubuk, and J. Gilmer, "A fourier perspective on model robustness in computer vision," in *NeurIPS*, 2019, pp. 13 255–13 265.

- [44] Y. Long, Q. Zhang, B. Zeng, L. Gao, X. Liu, J. Zhang, and J. Song, "Frequency domain model augmentation for adversarial attack," in *ECCV*, 2022.
- [45] A. Ilyas, L. Engstrom, and A. Madry, "Prior convictions: Black-box adversarial attacks with bandits and priors," in *ICLR*, 2019.
- [46] S. Moon, G. An, and H. O. Song, "Parsimonious black-box adversarial attacks via efficient combinatorial optimization," in *ICML*, vol. 97, 2019, pp. 4636–4645.
- [47] F. Schroff, D. Kalenichenko, and J. Philbin, "Facenet: A unified embedding for face recognition and clustering," in *CVPR*, 2015, pp. 815–823.
- [48] J. Deng, J. Guo, E. Ververas, I. Kotsia, and S. Zafeiriou, "Retinaface: Single-shot multi-level face localisation in the wild," in *CVPR*, 2020, pp. 5202–5211.
- [49] H. Wang, Y. Wang, Z. Zhou, X. Ji, D. Gong, J. Zhou, Z. Li, and W. Liu, "Cosface: Large margin cosine loss for deep face recognition," in *CVPR*, 2018, pp. 5265–5274.
- [50] J. Deng, J. Guo, N. Xue, and S. Zafeiriou, "Arcface: Additive angular margin loss for deep face recognition," in *CVPR*, 2019, pp. 4690–4699.
- [51] Z. Wang, A. C. Bovik, H. R. Sheikh, and E. P. Simoncelli, "Image quality assessment: from error visibility to structural similarity," *IEEE TIP*, vol. 13, no. 4, pp. 600–612, 2004.
- [52] R. Shin and D. Song, "Jpeg-resistant adversarial images," in *NIPSW*, vol. 1, 2017, p. 8.
- [53] W. Zhuang, Q. Chu, H. Yuan, C. Miao, B. Liu, and N. Yu, "Towards intrinsic common discriminative features learning for face forgery detection using adversarial learning," in *ICME*. IEEE, 2022, pp. 1–6.
- [54] C. Yu, X. Zhang, Y. Duan, S. Yan, Z. Wang, Y. Xiang, S. Ji, and W. Chen, "Diff-id: An explainable identity difference quantification framework for deepfake detection," *arXiv preprint arXiv:2303.18174*, 2023.